Analysis and impact of the Hunga Tonga-Hunga Ha'apai Stratospheric Water Vapor Plume

M. R. Schoeberl & Yi Wang, Science and Technology Corporation, Columbia, MD, USA

R. Ueyama, NASA Ames Research Center, Moffett Field, CA, USA

G. Taha, Morgan State University, Baltimore, MD, USA

E. Jensen, CIRES, Univ. of Colorado, Boulder, CO, USA

W. Yu, Hampton University, Hampton, VA, USA

Corresponding Author: Mark Schoeberl (mark.schoeberl@mac.com)

Key Points

- Hunga Tonga-Hunga Ha'apai eruption produced vertically overlapping but slightly displaced mid-stratospheric anomalies in H_2O and aerosols.
- IR cooling by enhanced H_2O layer explains the observed ~ 1.5K mid-stratospheric temperature decrease following the eruption.
- A simple model of the eruption H_2O enhancement combined with spreading of the plume explains the observations.

Plain Language Summary

Hunga Tonga-Hunga Ha'apai submarine volcano eruption on January 15, 2022 injected up to 150 Tg of water into the stratosphere. A month after eruption, a distinct aerosol and water vapor layer formed in the tropical southern hemisphere (SH) stratosphere. The water vapor layer is slightly displaced above the aerosol layer at 26 km. These two layers persisted in the tropical SH stratosphere over the next four months while slowly moving apart in altitude. The isolation of the layers and their separate motion are consistent with our understanding of tropical stratospheric dynamics. A cold temperature anomaly forms coincident with the water vapor layer, which we show to be due to enhanced IR radiative cooling by water vapor. Using a simple model, we show how the water vapor layer forms slightly above the aerosol layer.

Abstract

On Jan. 15, 2022, the Hunga Tonga-Hunga Ha'apai eruption injected SO_2 and H_2O into the middle stratosphere. The eruption produced a persistent mid-stratospheric sulfate aerosol layer, mostly below 26 km, confined to Southern Hemisphere (SH) tropics. Coincident with, and slightly above the aerosol layer, an enhanced H_2O layer is also observed. The SH tropical confinement is simulated using a trajectory model. Measurements over several months following the eruption show that the H_2O layer is slowly rising while the aerosol layer is descending. The H_2O layer upward movement is consistent with the vertical velocity at these altitudes. Gravitationally settling explains the descent of the aerosol layer. A cold anomaly coincident with the H_2O enhancement is observed and is caused by thermal adjustment to the additional H_2O IR cooling. A simple model of volcanic water injection at the time of the eruption simulates the observed H_2O.

Index Terms

0340 Middle atmosphere dynamics

0341 Middle atmosphere: constituent transport and chemistry

0370 Volcanic effects

1. Introduction

The Hunga Hunga-Tonga Ha'apai (HT) (20.54°S, 178.3°W) submarine volcano violently erupted on Jan. 15, 2022. Since HT was a submarine volcano, it appears to have lofted a significant amount of water into the stratosphere. Indeed, Microwave Limb Sounder (MLS) measurements show that HT water enhancement was quite high relative to SO_2 (Millán et al., 2022) – hereafter M22. The MLS estimated water injection was up to 146 Tg (M22). The eruption plume was detected up to 57 km (Carr et al., 2022; Proud et al., 2022). The Ozone Mapping and Profile Suite – Limb Profiler (OMPS-LP) detected extinction enhancements above 45 km (Taha et al., 2022).

In this paper we will examine at the evolution of the water vapor and aerosol enhancements that followed the HT eruption. M22 noted that the amount of water deposited in the stratosphere by HT was unprecedented in the modern history of volcanic eruption observations. Several MLS water vapor profiles made shortly after the eruption show concentrations exceeding 300 ppmv against a normal stratospheric concentration of ~4 ppmv. As the eruption evolved, MLS water vapor maps show that above about 2 hPa (~43 km), the plume quickly spreads and that the water vapor enhancement disperses. A secondary maximum at about 25 hPa (~26 km) persists (M22). The aerosol field shows similar behavior with rapid dispersal at higher altitudes but persistent high levels of aerosol extinction below ~ 25 hPa (~26 km) (Taha et al., 2022). The aerosol extinction in this layer grows over the 30 days following the eruption presumably due to the conversion of SO_2 to sulfate aerosols (e.g. Zhu et al., 2020).

There are several key questions concerning the HT eruption: Why did the unusual water vapor layer form and persist? Below we show that the water vapor enhancement overlaps the top of the extinction anomaly, but they are distinct, and furthermore the two enhancements vertically separate over time. We have also discovered a temperature anomaly in the 25-28 km region. We provide an explanation for the temperature anomaly as well as for the formation and evolution of the water vapor and aerosol layers.

2. Data sets

We use MLS v5 for ozone, temperature and H_2O, the quality of this data for the HT anomaly is discussed in M22. The MLS algorithm quality flags and convergence alerts were set for some plume profiles shortly after the eruption. Even with the quality flag and convergence filters set, the data looks reasonable and generally agrees with sonde and other validation data. For aerosols, we use OMPS-LP level-2 V2.1 745 nm extinction-to-molecular ratio data (AE) from all three OMPS-LP slits (see Taha et al., 2021). Taha et al. (2022) indicated that the standard V2.1 released data (used in this study) provides the most accurate aerosol retrieval up to 36 km. Thus, we restrict our constituent analysis to below 35 km which contains the main locus aerosol plume (Taha et al. 2022; Fig. 4). The MLS and OMPS-LP extinction data sets are averaged over 4 days and then averaged onto a 5° latitude-longitude grid.

To simulate the dispersal of the plume, we use the Forward Domain Filling (FDF) trajectory model (Schoeberl et al., 2018) modified to inject a dense column of parcels over the HT location on Jan 15, 2022. This simulation uses MERRA-2 reanalysis winds, temperatures, and heating rates (Gelaro, et al., 2017).

3. Analysis

Figure 1 shows the zonal mean distribution of water vapor and aerosol extinction ratio on Feb 15, 2022, a month after the eruption. The HT aerosol plume reaches 26 km in the region 30°S to about 5°N. The extinction data is quite sensitive to plumes extending outward from the tropics thus tends to show a wider distribution than the water vapor field. The water vapor plume is centered at 26 km and extends up to 30 km in the SH tropics. The water vapor plume mostly overlaps the aerosol plume while extending slightly above it.

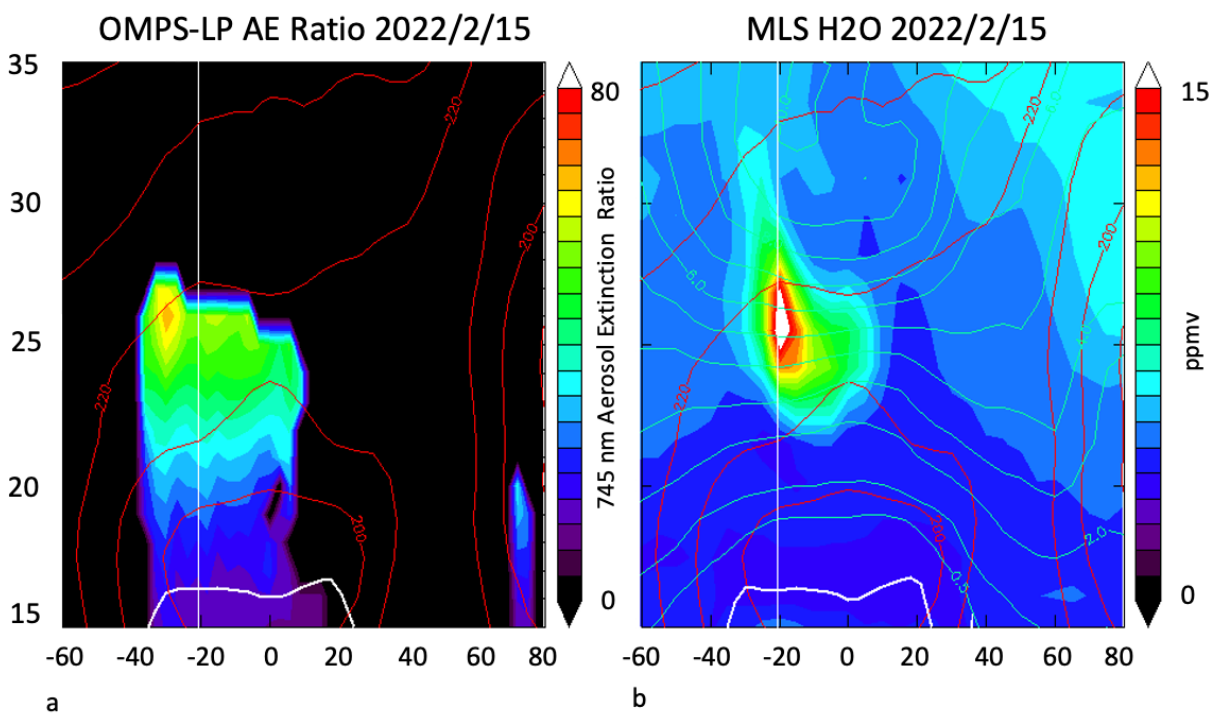

Figure 1 The zonal mean OMPS-LP 745 nm aerosol extinction/ molecular extinction ratio (Part a) and MLS water vapor (ppmv) (Part b) on Feb. 15, 2022. The red contours show the MLS temperature field. The thick white line is the zonal mean tropopause. The green contours are MLS ozone mixing ratio (ppm). The vertical white line denotes the latitude of the HT volcano.

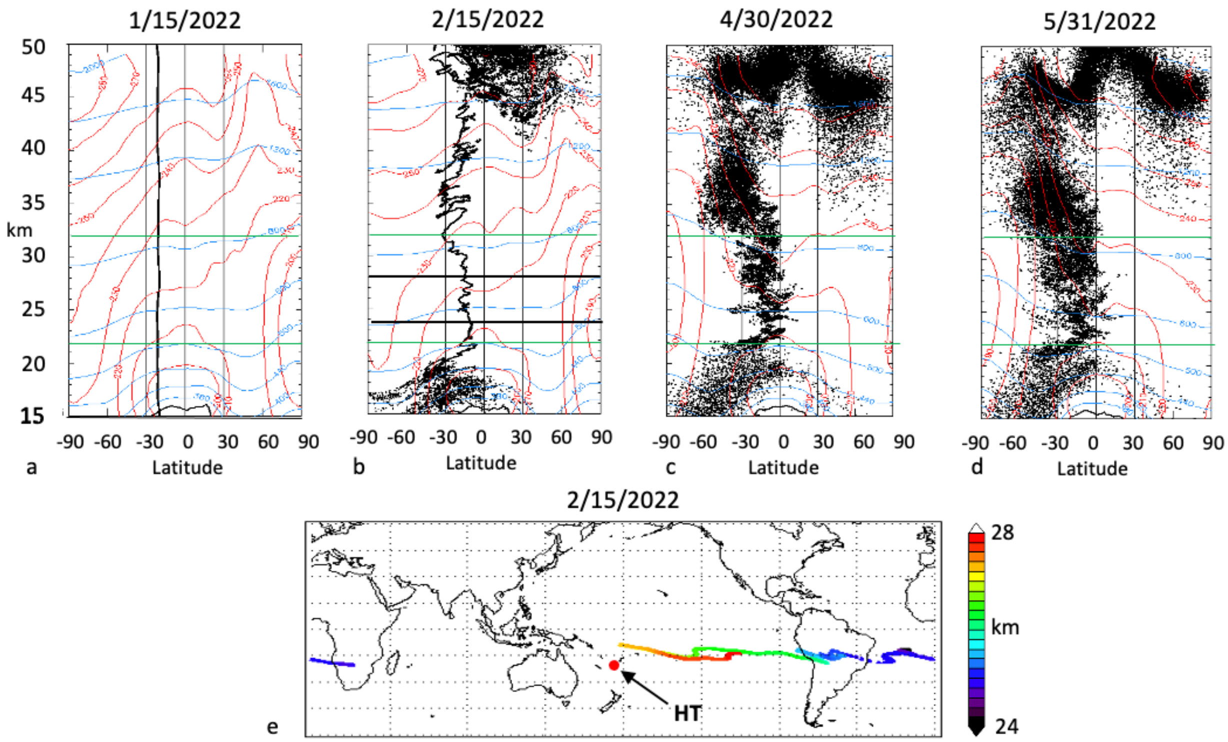

Figure 2 Dispersal of HT plume simulated by the FDF model: (Part a) shows the initial parcel distribution on Jan 15, (Part b) parcel distribution of Feb. 15, 2022, (Part c) shows the distribution at the end of April, and (Part d)shows the distribution at the end of May. Along the bottom (Part e), a map of parcels between 24-28 km with color scale indicating altitude. In Parts a,b,c,d red contours are MERRA-2 temperatures, blue contours are potential temperature. Horizontal green lines show the isolation region 22-32km. Horizontal black lines in Part b indicate the domain in Part e. The red dot locates HT on the map.

Figure 2 shows the dispersal of the plume using the FDF trajectory model. From the initial distribution (Fig. 2a), the plume evolves slowly and is mostly confined to the region between the equator and 30°S in the height range 22-32 km. This confinement is still somewhat evident at the end of April. The isolation of the Northern Hemisphere (NH) tropics from the Southern Hemisphere (SH) tropics in this region was first noted by Stolarski et al. (2014) when analyzing the interhemispheric phasing of the tropical ozone concentration. Below ~20 km parcels are dispersing mostly to the SH extra-tropics along the isentropes. Above about 35 km parcels are also drifting together into the SH. At highest altitudes, parcels are moving out of the tropics into the NH extra-tropics.

Timeseries of the zonal mean aerosols and water vapor at 15°S±2.5° are shown in Fig. 3a,b. We also plot the temperature anomaly (Fig. 3c) as a departure of the zonal mean MLS temperature on Jan 1 from the subsequent zonal mean temperatures. The perturbation heating rate shown is Fig. 3d is computed using the AER longwave radiative transfer model (Mlawer et al., 1997). The heating rate calculation uses MLS ozone, temperature, and water vapor. The anomaly is computed by fixing the water vapor to the pre-eruption profile and computing the heating rates over the period. We then subtract those heating rates from the heating rates computed using MLS observed water data.

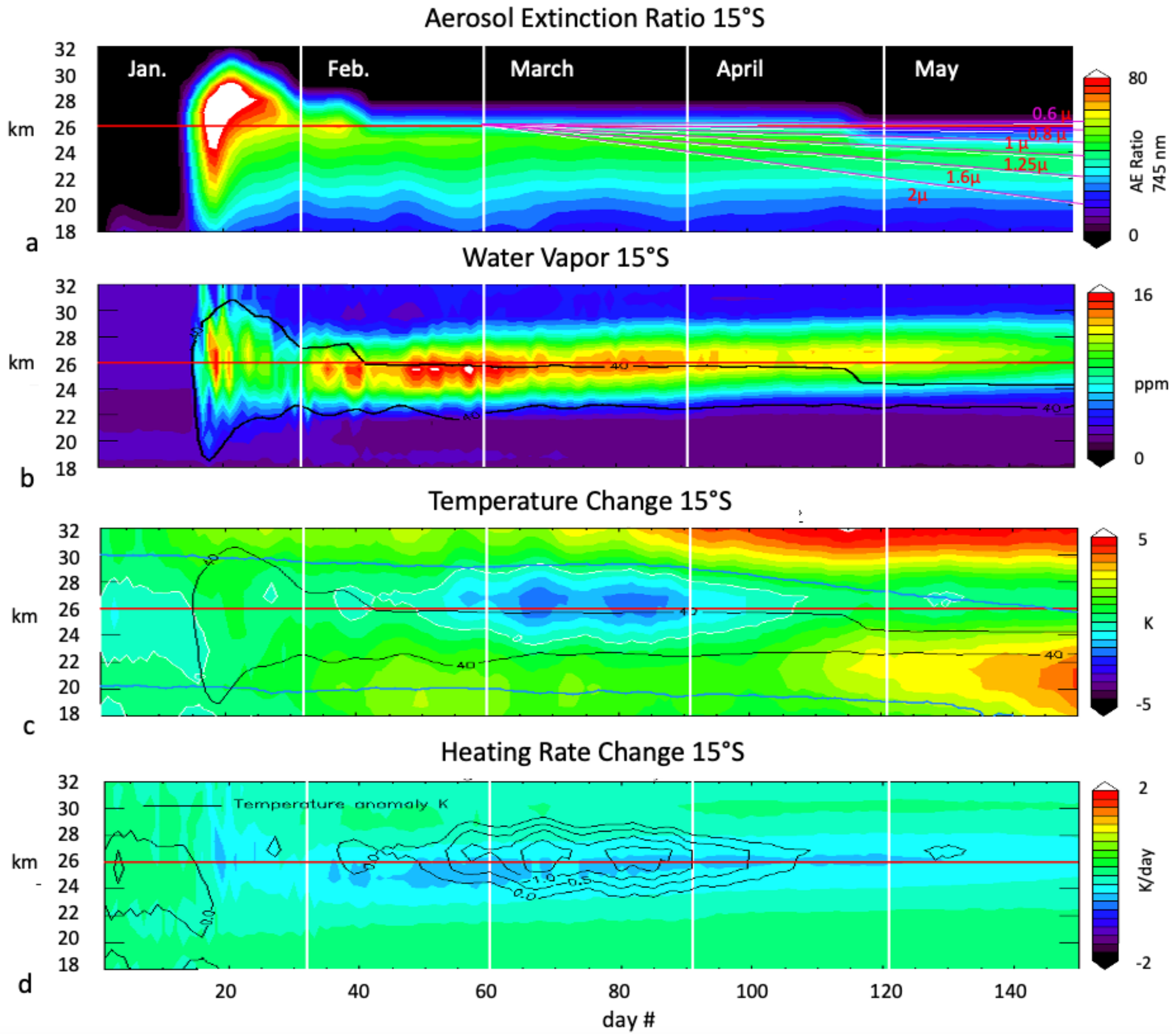

Figure 3 Times series of aerosol extinction ratio (AE) (Part a), water vapor (Part b), temperature anomaly (Part c), and heating rate anomaly (Part d) at 15°S. Parts b & c show black contours of 40 AE that outline the aerosol anomaly. In Part d, the heating rate anomaly has the Part c temperature contours superimposed. Pink lines in Part a represent the downward gravitational settling of aerosols of different diameters (μm) as labeled. Blue contours in Part c indicates the altitude of the zero zonal wind lines at the equator showing the descent of the QBO. The red line in all parts indicates 26km.

First, comparing the aerosol extinction field (Fig. 3a) with the water vapor (Fig. 3b), we see that the water vapor anomaly is slowly ascending whereas the aerosol concentration appears to be descending. The simple explanation for this effect is that the water vapor is transported upward with the diabatic circulation that gives rise to the tropical trace gas tape recorders (Schoeberl et al., 2008a) whereas the aerosols are gravitationally settling. The 26 km water vapor anomaly ascent rate is ~2 km over 80 days or ~0.028 cm/s. This vertical velocity is consistent with the velocity of 0.03±0.005 cm/s at 26 km estimated by Schoeberl et al. (2008b). Using 0.028 cm/sec as a background ascent velocity, Fig 3a shows the net settling rate for aerosols with different sizes after day 60 (Stokes formulas in Pruppacher et al. 1998). The change in the aerosol height appears to match the settling for aerosol modal diameter of ~0.8 – 1μm. Smaller particles are carried upward by the circulation into warmer, lower relative humidity environment, and will evaporate (Tsagkogeorgas et al., 2017).

Second, Fig. 3c shows a cold temperature anomaly that begins to appear in early to mid-February, and the anomaly magnitude is consistent with radiosonde measurements (Vömel et al., 2022). This temperature anomaly is approximately coincident with the change in the cooling rate (Fig. 3d; correlation of $r = 0.42$) due to enhanced water vapor. If we assume in the thermodynamic equation that the temperature change (ΔT) balances the change radiative heating (ΔH), $\Delta T \sim \alpha \Delta H$, then we compute a Newtonian cooling time scale (α^{-1}) of 5 days at 26 km. This time constant is consistent other estimates of the Newtonian cooling rate for this region (e.g. Newman and Rosenfield, 1997). Thus, the temperature changes observed in the mid stratosphere are a thermal adjustment to the increased IR cooling.

By mid-March, the descending QBO temperature anomaly is evident in temperature increase at 32 km as the westerly phase descends through this region. The equatorial zero wind line altitude is superimposed on Fig. 3c to indicate the descent (see https://acd-ext.gsfc.nasa.gov/Data_services/met/qbo/qbo.html).

Note that volcanic aerosols can also heat the stratosphere (Aubry et al., 2021 and references therein). Shortly after the eruption, sonde measurements show a < 2K increase in temperatures below 25 km that disappears by early February (Vömel et al., 2022). After February we see no evidence of a temperature change co-located with the aerosol layer probably because the dispersed aerosol layer is too attenuated.

Why does the water vapor anomaly extend above the aerosol anomaly? To explore this problem, we have constructed a very simple model of the HT plume. Initially, the eruption is propelled upward by the explosion and latent heat release by condensation of water vapor. The plume temperature is likely well above stratospheric ambient. Within days to weeks the plume shears out and plume temperature cools to ambient. First, we assume, for simplicity, that the amount of water vapor available is now limited by the saturation mixing ratio over ice; i.e. excess water forms ice particles that quickly fall out until the relative humidity is reduced to 100%. We then assume that the amount of HT water lofted decreases above the eruption centroid height in mid-February – prior to mid-February the system is still in adjustment. These assumptions define the available water. Finally, we assume that the volcanic cloud is ~ 950 km in diameter at 16 km (somewhat larger that the GOES-17 image from NASA Worldview, but not unrealistic). This area is assumed to expand with altitude, conserving mass. As in Fig. 2e, the eruption cloud stretches out in longitude. Thus, the mid-February MLS zonal mean water vapor is the available water in the eruption cloud reduced by the ratio of the initial eruption cloud area to the tropical zonal mean area.

The model uses the OMPS-LP mid-February aerosol extinction profile (Fig. 1a) to set the eruption centroid height. We center a Gaussian distribution of erupted material at the centroid. The temperature profile at 20°S is shown in Fig. 4a along with the saturation mixing ratio over ice (Murphy and Koop, 2005). Below the eruption centroid, the ice amount is equal to the saturation mixing ratio; above the centroid the amount of water available is the saturation mixing ratio times the normalized by the Gaussian centroid. We add the observed background pre-eruption zonal mean MLS water vapor profile for realism. Fig. 4b shows the assumed eruption available water vapor profile and relative humidity on Feb 15 using centroid height of 26 km and a Gaussian standard deviation of 0.65 km. The available water reaches 600 ppmv at 26 km. MLS did observe the water vapor mixing ratios over 300 ppm at 26 km Jan. 16 (M22) and there are sonde measurements of even higher mixing ratios in this stratospheric region (Vömel et al., 2022).

The Feb. 15 zonal mean water vapor field (Fig. 4c) is assumed to be 15° wide from 5°S to 20°S and consists of the diluted plume shown in Fig. 3b. Fig. 4c also shows the observed aerosol extinction profile. The extinction profile is only used to verify the height of the eruption centroid and its width. The water vapor profile shows good agreement with zonal mean MLS data at 15°S. The extension of the water plume above the aerosol plume is also reproduced. The Fig 4c column water vapor mass above 100 hPa is 32.8 Tg; the MLS mass is 31.2 Tg.

In summary, the simple model requires three factors to explain the water vapor anomaly that extends above the aerosol anomaly: (1) the change in the saturation mixing ratio with altitude a controlled by the tropical temperature profile, (2) a decrease in volcanic water injection above the eruption centroid altitude, and (3) spatial dilution of the eruption plume. \

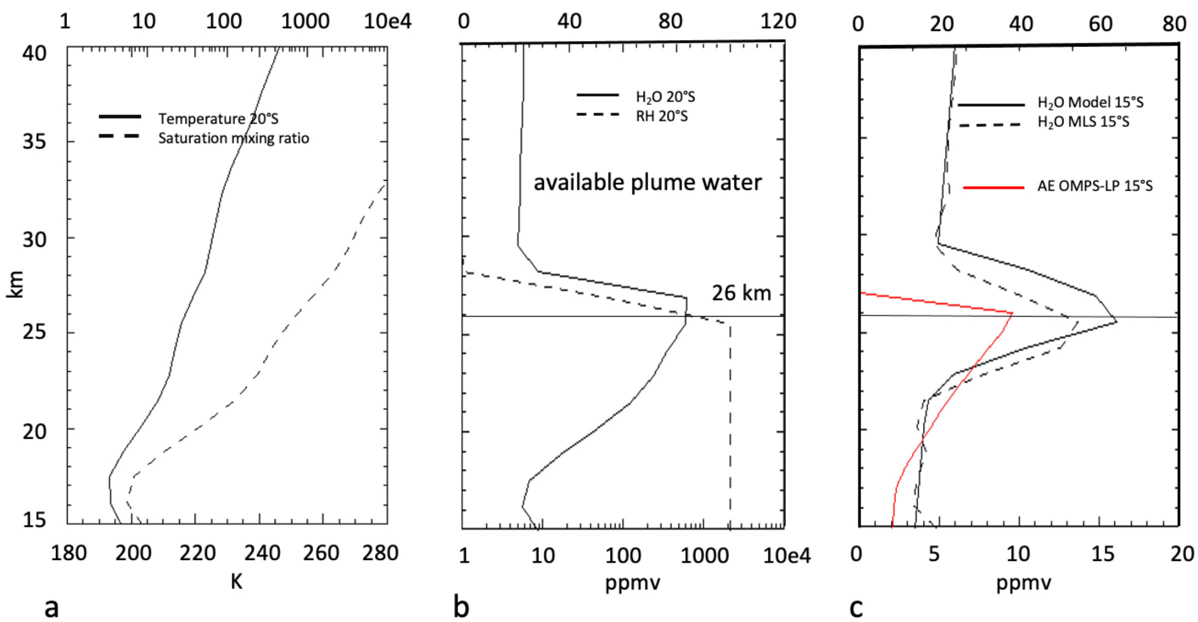

Figure 4 Model of HT water vapor injection. Part a shows Jan 15, 2022 temperature and saturation mixing ratio profile at the location of HT (20°S). Part b shows a model of the eruption available water vapor and relative humidity. Black lines for centroid at 26 km. Part c shows the zonal mean aerosol extinction ratio profile for Feb. 15, 2022 (red). Zonal mean water vapor profile (black) for the model and MLS zonal mean water vapor (dashed).

5. Summary and Discussion

The HT volcanic eruption produced stratospheric enhancements of both water and aerosols (sulfate after SO_2 oxidation). Our analysis shows that the aerosol and water vapor enhancements persisted from Jan 15 to May 31, 2022. Between 22-32 km the enhancements are confined mostly to the SH tropics as is evident from observations and consistent with a trajectory analysis. This isolation of the stratospheric SH tropics from the NH tropics is consistent with tropical ozone observations (Stolarski et al., 2014). Below about 20 km, the aerosol observations and trajectory analyses show that aerosols and water mostly disperse out of the SH tropics. The trajectories suggest that most of the aerosols move to the SH with a smaller amount moving into the NH. Above 40 km the trajectory model suggests that eruption material moves into the Northern Hemisphere as part of the cross-hemispheric upper stratospheric circulation (Schoeberl and Strobel, 1978; Holton and Wehrbein, 1980).

By mid-February, the tropical mid-stratosphere aerosol and water vapor enhancements are slightly offset from each other, with the water vapor anomaly about 1 km higher. The two distinct layers continue separate over the 4 ½ month period after the eruption. The ascent speed of the water vapor anomaly is consistent with the magnitude of the upward branch of the large scale diabatic circulation. The descent of the aerosol layer is consistent with the gravitational settling of particles between 0.6 and 1 μm. Smaller particles will be carried upward and evaporate.

Tropical temperatures at 26 km, 15°S show anomalous decrease about a month after the eruption at the water vapor enhancement altitude. This temperature decrease is also seen in sonde measurements (Vömel et al., 2022). IR radiative transfer computations show that the temperature decrease is associated with enhanced water vapor IR cooling as might be expected (de F. Forster and Shine, 1999). The Newtonian cooling rate calculated from observed temperature and cooling rate changes is consistent with previous computations (Newman and Rosenfield, 1997).

To explore the formation of the water vapor anomaly, we use a simple model of the eruption. In the model we define an eruption centroid altitude, we assume that there is a decreasing amount of water injected above that altitude and the relative humidity below that altitude is 100%. The water vapor then disperses zonally. Our model water vapor matches the zonal mean MLS measurements one month after the eruption and is consistent with the range of MLS H_2O measurements made shortly after the eruption (M22).

Our simple model suggests that even larger water vapor anomalies would have formed if the volcanic eruption had lofted water into higher, warmer stratospheric air. On the other hand, smaller water vapor anomalies would have occurred for lower altitude injections or higher latitude injections into colder stratospheric air. This, along with the fact that most volcanic eruptions in the recent past were not submarine may explain why water vapor enhancements have not been as evident in previous eruptions (M22).

Acknowledgements
This work was supported under NASA grant NNX14AF15G, and 80NSSC21K1965. The authors would like to thank Natalya Kamarova for discussions.

Open Research

MERRA-2 Reanalysis data. Gelaro et al. (2017). MERRA-2 data are obtained from the Global Modeling and Assimilation Office (GMAO), *inst3_3d_asm_Cp: MERRA-2 3D IAU State, Meteorology Instantaneous 3-hourly (p-coord, 0.625x0.5L42), version 5.12.4* at https://doi.org/10.5067/WWQSXQ8IVFW8. Data is public, unrestricted access (registration required).

OMPS-LP data, Taha et al. (2021), is available at https://disc.gsfc.nasa.gov/datasets/OMPS_NPP_LP_L2_AER_DAILY_2/summaryDOI: 10.5067/CX2B9NW6FI27. The algorithm is documented in. Data is public, unrestricted access (registration required).

Aura MLS Level 2 data, Livesey et al. (2017) JPL D-33509 Rev. C, is available at https://disc.gsfc.nasa.gov/datasets?page=1&keywords=AURA%20MLS; Aura MLS Derived Meteorological Products (DMPs): https://mls.jpl.nasa.gov/eos-aura-mls/dmp (registration required).

References

Aubry, T. J., J. Staunton-Sykes, L. R. Marshall, J. Haywood, N. L. Abraham & A. Schmidt, (2021)/Climate change modulates the stratospheric volcanic sulfate aerosol lifecycle and radiative forcing from tropical eruptions, Nature Comm., 12:4708 https://doi.org/10.1038/s41467-021-24943-7

Carr, J. L., Horvath, A., Wu, D. L., & Friberg, M. D. (2022). Stereo plume height and motion retrievals for the record-setting Hunga Tonga-Hunga Ha'apai eruption of 15 January Geophysical Research Letters. doi:10.1029/2022GL098131

de F. Forster, Piers M., Shine, Keith P. (1999) Stratospheric water vapour changes as a possible contributor to observed stratospheric cooling. Geophysical Research Letters, 26 (21). 3309-3312 doi:10.1029/1999gl010487

Gelaro, R., et al. (2017), The Modern-Era Retrospective Analysis for Research and Applications, Version 2 [Dataset], J. Climate, 30, 5419-5454, https://doi.org/10.1175/jcli-d-16-0758.1.

Holton, J. R. and W. M. Wehrbein (1980), A numerical model of the zonal mean circulation of the middle atmosphere, Pure and Appl. Geophys., 119, 284-306.

Millán, L. et al., (2022). The Hunga Tonga-Hunga Ha'apai Hydration of the Stratosphere, Geophysical Research Letters. (submitted) doi:10.1002/essoar.10511266

Mlawer, E.J., S.J. Taubman, P.D. Brown, M.J. Iacono and S.A. Clough: RRTM, a validated correlated-k model for the longwave. *J. Geophys. Res*., **102**, 16,663-16,682, 1997.

Newman, P. A. and J. E. Rosenfield (1997). Stratospheric thermal damping times, Geophys. Res. Lett., 24, 433-436.

Murphy, D. M. and T. Koop (2005), Review of the vapour pressures of ice and supercooled water for atmospheric applications, Quart. J. Royal Met. Soc, 131, 1539-1565.

Proud, S. R., Prata, A., & Schmauss, S. (2022). The January 2022 eruption of Hunga Tonga-Hunga Ha'apai volcano reached the mesosphere. Earth and Space Science Open Archive, 11. Retrieved from https://doi.org/10.1002/essoar.10511092.1 doi: 10.1002/essoar.10511092.1

Pruppacher, H. R., J. D. Klett & P. K. Wang (1998). *Microphysics of Clouds and Precipitation*, 28:4, 381-382, doi: 10.1080/02786829808965531

Schoeberl, M. R. and D. F. Strobel, (1978). The Zonally Averaged Circulation of the Middle Atmosphere, *J. Atmos. Sci.,* **35**, 577-591.

Schoeberl, M. R. et al., (2008a) QBO and annual cycle variations in tropical lower stratosphere trace gases from HALOE and Aura MLS observations, J. Geophys. Res, VOL. 113, D05301, https://doi.org/10.1029/2007JD008678

Schoeberl, M. R., A. R. Douglass, R. S. Stolarski, S. Pawson, S. E. Strahan, and W. Read (2008b), Comparison of lower stratospheric tropical mean vertical velocities, J. Geophys. Res., 113, D24109, doi:10.1029/2008JD01022

Schoeberl, M. R., Jensen, E. J., Pfister, L., Ueyama, R., Avery, M., & Dessler, A. E. (2018), Convective hydration of the upper troposphere and lower stratosphere, J. of Geophys. Res.: Atmospheres, 123, 4583–4593, https://doi.org/10.1029/2018JD028286.

Stolarski, R. S., D. W. Waugh, L. Wang, L. D. Oman, A. R. Douglass, and P. A. Newman (2014), Seasonal variation of ozone in the tropical lower stratosphere: Southern tropics are different from northern tropics, J. Geophys. Res. Atmos., 119, 6196–6206, doi:10.1002/ 2013JD021294.

Taha, G., R. Loughman, T. Zhu, L. Thomason, J. Kar, L. Rieger, and A. Bourassa (2021), OMPS LP Version 2.0 multi-wavelength aerosol extinction coefficient retrieval algorithm, Atmos. Meas. Tech., 14, 1015–1036, https://doi.org/10.5194/amt-14-1015-2021

Taha, G., R. Loughman, P. Colarco, T. Zhu, L. Thomason, G. Jaross (2022), Tracking the 2022 Hunga Tonga-Hunga Ha'apai aerosol cloud in the upper and middle stratosphere using space-based observations, Geophysical Research Letters. (submitted).

Tsagkogeorgas et al. (2017), Evaporation of sulfate aerosols at low relative humidity, Atmos. Chem Phys, 17,8923-8938, https://doi.org/10.5194/acp-17-8923-2017.

Vömel, H., S. Evan, and M. Tully (2022), Hunga Tonga-Hunga Ha’apai injects unprecedented amounts of water vapor into the stratosphere, Science, submitted.

Zhu, Y., Toon, O. B., Jensen, E. J., Bardeen, C. G., Mills, M. J., Tolbert, M. A., Yu, P., and Woods, S.: Persisting volcanic 715 ash particles impact stratospheric SO_2 lifetime and aerosol optical properties, Nat. Comm., 11, 4526, https://doi.org/10.1038/s41467-020-18352-5, 2020.